Cardiovascular Research (2016) **109**, 419–430
doi:10.1093/cvr/cvw005

Genetic lineage tracing discloses arteriogenesis as the main mechanism for collateral growth in the mouse heart

Lingjuan He[1], Qiaozhen Liu[1], Tianyuan Hu[1], Xiuzhen Huang[1], Hui Zhang[1], Xueying Tian[1,2], Yan Yan[3], Li Wang[4], Yu Huang[4], Lucile Miquerol[5], Joshua D. Wythe[6], and Bin Zhou[1,2,7]*

[1]Key Laboratory of Nutrition and Metabolism, Institute for Nutritional Sciences, Shanghai Institutes for Biological Sciences, Graduate School of the Chinese Academy of Sciences, Chinese Academy of Sciences, Shanghai 200031, China; [2]Institute of Neuroscience, State Key Laboratory of Neuroscience, CAS Center for Excellence in Brain Science and Intelligence Technology, Shanghai Institutes for Biological Sciences, Chinese Academy of Sciences, Shanghai 200031, China; [3]Zhongshan Hospital, Fudan University, Shanghai 200032, China; [4]Institute of Vascular Medicine, Shenzhen Research Institute, and Li Ka Shing Institute of Health Sciences, Chinese University of Hong Kong, Hong Kong, China; [5]Aix Marseille Universite, CNRS, IBDM UMR 7288, Marseille 13288, France; [6]Department of Molecular Physiology and Biophysics, Cardiovascular Research Institute, Baylor College of Medicine, Houston, TX 77030, USA; and [7]ShanghaiTech University, Shanghai 201210, China

Received 21 July 2015; revised 27 November 2015; accepted 29 December 2015; online publish-ahead-of-print 13 January 2016

Time for primary review: 27 days

Aims Capillary and arterial endothelial cells share many common molecular markers in both the neonatal and adult hearts. Herein, we aim to establish a genetic tool that distinguishes these two types of vessels in order to determine the cellular mechanism underlying collateral artery formation.

Methods and results Using Apln-GFP and Apln-LacZ reporter mice, we demonstrate that APLN expression is enriched in coronary vascular endothelial cells. However, APLN expression is reduced in coronary arterial endothelial cells. Genetic lineage tracing, using an Apln-CreER mouse line, robustly labelled capillary endothelial cells, but not arterial endothelial cells. We leveraged this differential activity of Apln-CreER to study collateral artery formation following myocardial infarction (MI). In a neonatal heart MI model, we found that Apln-CreER-labelled capillary endothelial cells do not contribute to the large collateral arteries. Instead, these large collateral arteries mainly arise from pre-existing, infrequently labelled coronary arteries, indicative of arteriogenesis. Furthermore, in an adult heart MI model, Apln-CreER activity also distinguishes large and small diameter arteries from capillaries. Lineage tracing in this setting demonstrated that most large and small coronary arteries in the infarcted myocardium and border region are derived not from capillaries, but from pre-existing arteries.

Conclusion Apln-CreER-mediated lineage tracing distinguishes capillaries from large arteries, in both the neonatal and adult hearts. Through genetic fate mapping, we demonstrate that pre-existing arteries, but not capillaries, extensively contribute to collateral artery formation following myocardial injury. These results suggest that arteriogenesis is the major mechanism underlying collateral vessel formation.

Keywords Apln-CreER • Lineage tracing • Collateral artery • Arteriogenesis • Arterialization

1. Introduction

Coronary artery disease is the leading cause of mortality and morbidity worldwide. Elucidating the mechanisms underlying coronary vessel growth in both healthy and pathological contexts (such as myocardial injury) may greatly aid future therapeutic angiogenic strategies in clinical settings. In patients with ischaemic vascular disease, collateral arteries develop as a compensatory mechanism to sustain functional blood flow, and the presence of this functional bypass, usually detected by angiography, has been associated with fewer ischaemic complications and diminished angina pectoris.[1] Currently, there are two models explaining collateral artery formation.[2] The first model, arteriogenesis,

* Corresponding author. Tel: +86 21 54920974; fax: +86 21 54920974, Email: zhoubin@sibs.ac.cn

posits that visible collateral arteries are formed from pre-existing arteries by rapid lumen opening and vascular wall thickening.[3] Arteriogenesis is a widely accepted model for explaining collateral artery formation.[4–6] The collateral artery formed through arteriogenesis becomes a large size (diameter) artery that is critical for supplying oxygenized blood to the ischaemic myocardium, which may account for the recovery and survival of the myocardium following a heart attack. In fact, studies have shown that a large collateral artery conducts blood flow more efficiently than angiogenesis.[7] A second, alternative model explaining collateral vessel growth is the *de novo* formation of collateral arteries from capillary beds through angiogenesis followed by vessel remodelling and the subsequent recruitment of pericytes and smooth muscle cells (SMCs) in a process known as arterialization.[8,9] The coalescence of the coronary capillaries to form the mature coronary arteries during embryogenesis is just one example of arterialization.[10] In the setting of post-natal or adult injury, arterialization usually refers to angiogenic capillaries giving rise to small size arteries in the ischaemic region of heart induced by hypoxia, whereas shear stress is classically thought to drive arteriogenesis. At the molecular level, arterialization requires the activity of the hypoxia-induced mitogen and cell signalling ligand vascular endothelial growth factor (VEGF) in ischaemic regions, whereas arteriogenesis is not associated with increased expression of VEGF or other hypoxia-inducible genes.[11] Determining the extent to which these two distinct mechanisms function to sustain coronary blood flow in normal and pathological settings is critical for our understanding of vascular biology and is a necessity for future therapeutic advances targeting neovascularization for treatment of ischaemic diseases.

One characteristic shared by both arteriogenesis and arterialization is the presence of mature, patent collateral arteries after injury. Due to the limited resolution of angiography, the inherit lack of information available from static histological analyses, and a paucity of appropriate genetic lineage labelling tools, a definitive determination of whether mature collateral arteries arise from pre-existing arteries (arteriogenesis) or from capillaries (arterialization) has been challenging (if not impossible).[1,12,13] Essentially, an angiogram (or histological analyses) showing an increased number of visible collateral arteries following an injury cannot distinguish between these two mechanisms to determine how the collateral arteries are formed.[1,13] Thus, the ability to differentiate between these two vascular beds is a prerequisite for determining which mechanism accounts for collateral vessel formation. Identification of a molecular marker that is differentially expressed in arteries and capillaries may enable the determination of which of these two models is primarily utilized during ischaemic responses.

Apelin (Apln) encodes a highly conserved peptide of 77 amino acids and is the endogenous ligand for the human orphan G protein-coupled receptor, APJ.[14] Expression of APJ and Apln is highly enriched in the cardiovascular system, and they play crucial physiological roles in the regulation of both cardiac contractility and blood pressure.[15,16] Expression of Apln is regulated by hypoxia, and ischaemia-induced hypoxic stimuli increase Apln transcription, which in turn regulates vascular endothelial cell proliferation and regenerative angiogenesis.[17] Mechanistically, Apln expression and secretion within the heart are regulated by the hypoxia-inducible transcription factor pathway in cardiomyocytes.[18] A proangiogenic role for Apln is also conserved in both embryonic and tumour angiogenesis.[19] Interestingly, Apln also promotes haematopoiesis in human embryonic stem cells *in vitro*[20] and functions as a potent chemoattractant to recruit circulating APJ^+ cells during myocardial repair *in vivo*, which may provide myocardial protection against ischaemic damage by improving neovascularization via a paracrine signalling mechanism.[21] Apln expression is typically low in the adult vasculature, but in response to hypoxia, under ischaemic conditions such as myocardial infarction (MI) or within a tumour, Apln expression is robustly increased, particularly during sprouting angiogenesis.[19] In fact, our recent work showed that an Apln-CreER mouse line distinguishes sprouting, angiogenic vessels from stable, quiescent endothelium in both MI and tumour angiogenesis models in the adult mouse.[22] Here we unexpectedly find that Apln is also expressed differentially between capillary and arterial endothelial cells. We demonstrate that although Apln is indeed expressed in capillary vessels, it is notably absent from the coronary arteries in the neonatal heart. Furthermore, we find a similar pattern of expression in the adult heart following MI. Taking advantage of this distinction, we used Apln-CreER-mediated genetic lineage tracing to delineate the cellular mechanism for collateral artery formation during MI.

2. Methods

2.1 Mice

All animal procedures were performed conform the guidelines from Directive 2010/63/EU of the European Parliament on the protection of animals used for scientific purposes; experimental protocol was approved by the Institutional Animal Care and Use Committee of the Institute for Nutritional Sciences, Shanghai Institutes for Biological Sciences, Chinese Academy of Sciences (approved protocol number 2015-AN-8). All efforts were made to minimize suffering in animals. Mice were sacrificed by CO_2 and tissues were collected afterwards for analyses. The Apln-GFP knock-in line was generated by homologous recombination using Red/ET recombineering,[23] with the knock-in strategy replacing the endogenous ATG with a cDNA encoding a GFPCre fusion. Long-distance PCR, spanning the 5′ and 3′ homology arms, was used to screen targeted embryonic stem cell clones. Correctly targeted clones were used for blastocyst injection into pseudo-ovulated females by Shanghai Biomodel Organism Co., Ltd. China.Apln-CreER, Apln-LacZ, CX40-GFP, and Rosa26-RFP mice were described previously[24–27] and maintained on an ICR/C57BL6/J-mixed background. Tamoxifen (Sigma) was dissolved in corn oil (20 mg/mL) and administered by oral gavage at the indicated time (0.1–0.15 mg tamoxifen/g mouse body weight).

2.2 Neonatal MI

Neonatal MI was performed as described previously.[28] Briefly, neonatal pups were anaesthetized by cooling on a bed of ice. After pups were not responsive to external stimuli, their chests were disinfected with iodine. A longitudinal incision of 0.3–0.5 cm was made in the sternum (between the second and third ribs), and the heart was exposed through the left thoracotomy. The left anterior descending (LAD) coronary artery was permanently occluded with an 11-0 non-absorbable suture. Afterwards, the thoracic wall incisions were closed with an 8-0 absorbable suture, and the skin wound closed using an 11-0 suture. After surgery, the neonates were removed from the ice bed and put below a 37°C heat lamp for recovery. Sham-operated mice underwent the same procedure involving hypothermic anaesthesia and thoracotomy, but without ligation of their LAD coronary artery.

2.3 Adult MI

Adult mice were subjected to surgical manipulation as described previously.[22] The ventilator respiratory rate was set between 120 and 130, and the respiratory volume to 0.3–0.5 mL. Anaesthesia was induced by tracheal intubation and administration of 2% isoflurane gas while the core temperature of the animal was maintained by placement upon a 37°C water-heated pad. Upon reaching a surgical plane of anaesthesia, the isoflurane concentration was adjusted to 1.5%. We confirmed that the mice

were ready for surgery by pain reflex reaction (lack of response to hind limb toe pinch). The limbs were then fixed in place and their chest skin disinfected. A vertical 1–1.5 cm incision was made at the sternum, and then a blunt dissection of the muscle and fascia was performed to avoid injuring the blood vessels. After making an ~1 cm incision between the third and fourth intercostal ribs, the chest was expanded to ~0.8 cm wide. Then the LAD branch of the coronary artery was permanently ligated with a 0-8 suture. The ligation was judged as successful when the heart showed signs of cyanosis. The incisions were closed with a 6-0 suture, and any bubbles were discharged from the chest. The surgical incision was disinfected and mice were supplied with pure oxygen for 4–5 min until they resumed spontaneous breathing. Then the tracheal intubation tube was removed and the mice were kept warm until recovery of normal behaviour was observed, followed by treatment with analgesics.

2.4 Immunohistochemistry

Immunostaining was performed as previously described.[29] Briefly, hearts were collected in phosphate-buffered saline (PBS) on ice and then fixed in 4% paraformaldehyde at 4°C for 1 h. After washing in PBS, tissues were incubated in PBS/30% sucrose overnight at 4°C and embedded in optimum cutting tissue (OCT, Sakura) and snap frozen the following day. Cyrosections of 10 μm thickness were collected on positively charged slides. Tissues were blocked with PBS/0.1% Triton X-100/5% normal donkey serum (Jackson ImmunoResearch) for 1 h at room temperature, followed by primary antibody incubation overnight at 4°C. Signals were visualized with Alexa fluorescence-conjugated secondary antibodies (Invitrogen). For weak signals, we used horseradish peroxidase- or biotin-conjugated secondary antibodies and a tyramide signal amplification kit (PerkinElmer). Antibodies used were as follows: PECAM/CD31 (BD Pharmingen), Smooth muscle actin (Sigma), RFP (Rockland), GFP (Invitrogen), VE-CAD (R&D), and Estrogen receptor (Abcam). Images were acquired using an Olympus confocal microscope (FV1000), a Zeiss confocal microscope (LSM510), or a Leica M165 FC stereo microscope. The quantification of all experiments was performed by an observer blinded to the experimental design.

2.5 Histology (Sirius Red and Masson's trichrome)

Histology was performed as described previously.[30] Briefly, mouse hearts were fixed in 4% paraformaldehyde overnight at room temperature. In the following day, hearts were dehydrated through a series of 70, 80, 95, and 100% ethanol for 30 min, then moved into butyl alcohol for 2 h, and embedded with paraffin (Leica). Paraffin sections (10 μm), spanning the entire heart, were cut using a rotary microtome. Sections were de-waxed in xylene two times and rehydrated by a series of 100, 95, 80, and 75% ethanol:ddH_2O and fixed in Bouin's solution (5% acetic acid, 9% formaldehyde, and 0.9% picric acid) for 12–24 h at room temperature. For Sirius Red staining, sections were stained by 0.1% fast green for 10–15 min, treated with 1% acetic acid for 2 min, stained by 0.1% Sirius Red for 20 min, then serially dehydrated in ethanol and xylene, and mounted in Permount™ Mounting Medium. For Trichrome staining, sections were incubated in Weigert's haematoxylin for 10 min, blued under running tap water for 5 min, and then incubated in Biebrich Scarlet for 5 min. Afterwards, sections were treated with phosphotungstic/phosphomolybdic acid for 10 min and then directly transferred into aniline blue for 5 min, and then moved into 1% acetic acid for 1 min. The sections were then dehydrated by an ethanol series and xylene and then mounted in Permount Mounting Medium. Images were acquired on either a Leica M165 FC stereo microscope or an Olympus BX53 microscope.

2.6 X-gal staining

X-gal staining was performed as described previously.[24] Briefly, hearts were collected in PBS on ice and then fixed in 4% paraformaldehyde at 4°C for 1 h. After washing in PBS, hearts were incubated with 30% sucrose overnight at 4°C, and the following day they were embedded in OCT (Sakura) and snap frozen. Cryosections of 10 μm thickness were collected on positively charged slides. Sections were washed in PBS three times and treated with LacZ stain solution at 37°C for 3–4 h. After additional PBS washes, slides were mounted in 50% glycerol. X-gal staining was followed by immunochemistry (according to standard protocols). Images were acquired using an Olympus BX53 microscope.

2.7 TTC staining

TTC (2,3,5-triphenyltetrazolium chloride) staining was performed as described.[30] Briefly, mouse hearts were harvested at 3–6 h after MI and then washed in PBS three times. Hearts were then incubated in 0.5% TTC solution for 30 min, then transferred to 10% formalin, and incubated for 20 min at room temperature. Hearts were then washed in PBS three times. Images were acquired on a Leica M165 FC stereo microscope.

2.8 Microfil angiography

A solution of PBS and heparin (1 : 10 dilution) was intraperitoneally injected into the abdomen of the mouse. After 5 min, the mice were euthanized and their chest was opened to visualize the great vessels. Microfil (Flow Tech Incorporation, MA, USA) was then injected into the left ventricle by syringe until the coronary vessels were filled. After the casting material had completely hardened, the perfused organ was removed and placed in sodium hydroxide solution for several days. The cast was then rinsed several times in water until all the digested tissue was removed. A detailed protocol can be found at www.flowtechinc.com. Images were acquired on a Leica M165 FC stereo microscope.

2.9 Echocardiography

Anaesthetized mice were subjected to transthoracic echocardiography using a Vevo770 micro-ultrasound system (VisualSonics; Toronto, Canada). All measurements were performed 28 days after MI or sham operation on mice sedated by administration of 2% isoflurane via nosecone inhalation. Percentage changes of both left ventricular ejection fraction (EF%) and fractional shortening (FS%) were calculated for both MI and sham-operated mice.

2.10 Apln expression and shear force stress experiments

Human umbilical vein endothelial cells (ATCC) were seeded on glass slides (75 mm × 38 mm; Corning) coated with fibronectin (50 μg/mL). After 16 h of incubation, the cells were changed to medium containing 2% foetal bovine serum for 6 h. The slides were mounted in a custom-built flow chamber and connected to the IBIDI Flow system. About 12 dyn/cm^2 laminar shear force was applied for different temporal durations (4, 8, and 16 h, respectively). Total RNA was extracted (Trizol) and cDNA was transcribed (Superscript III kit, Invitrogen) for quantitative real-time PCR (qRT-PCR). Relative Apln mRNA expression levels were compared with static conditions (no shear force condition). Gene expression was normalized to Gapdh transcript levels. Apln primers used for qRT-PCR were: forward, TCCCAAATCGGTTCTAGGTC; reverse, CCTGTAAGTGGGCTGGATTT. Gapdh primers used for qRT-PCR were: forward, TGCACCACCAACTGCTTAGC; reverse, GGCATGGACTGTGGTCATGAG.

2.11 Statistics

Data for two groups were analysed by an unpaired Student's *t*-test, whereas comparison between more than two groups was performed using an analysis of variance followed by Tukey's multiple comparison test. Significance was accepted when $P < 0.05$. All data are presented as mean ± SEM.

3. Results

3.1 APLN is expressed in capillary but not arterial endothelial cells in the neonatal mouse heart

Both artery and capillary vessels contain an endothelial cell layer, and the endothelial cells of these two types of vessels share many common molecular markers, such as Tie1, Tie2, Flk1, and VE-cadherin (Cdh5).[31] Genetic mouse lines that express Cre recombinase under the control of a pan-endothelial cell enhancer or promoter sequences (e.g. Tie1-Cre, Tie2-Cre, Flk1-Cre, and VE-Cadherin/Cdh5-Cre) have significantly advanced our understanding of developmental and pathological vasculogenesis and angiogenesis.[32–38] However, currently, there is no genetic tool that can distinguish between the endothelial cells of these two types of major blood vessels. Identification of a molecular marker that differentially labels arterial or capillary endothelial cells, and the generation of genetic tools based on such a novel marker, would greatly facilitate future investigations into the cellular and molecular mechanisms controlling vascular development and disease.

Apln is present in most vascular endothelial cells during embryogenesis, but it is lowly expressed in the endocardium and great vessels (aortic endothelium) of the developing mouse heart.[24,39] Unlike the Apln^{+} preliminary coronary capillary plexus present at E11.5–E14.5, the Apln^{-} endothelial cells in the aorta are associated with SMCs.[10,24,40] This observation prompted us to determine whether Apln expression was also diminished or absent in mature arteries of the post-natal heart, as they too are associated with and in intimate proximity to SMCs. By microfil injection, we could identify functional coronary arteries in the neonatal heart (*Figure 1A*). We used two immunohistochemical markers to label coronary arteries: alpha smooth muscle actin (SMA) to label SMCs and Connexin 40 (Cx40^{+})[27] to mark arterial endothelial cells (Supplementary material online, *Figure S1*). To monitor Apln expression in the neonatal hearts, we generated a novel Apln-GFP knock-in mouse line, in which a cDNA encoding a GFPCre fusion was inserted into the endogenous Apln locus, replacing the translational start codon

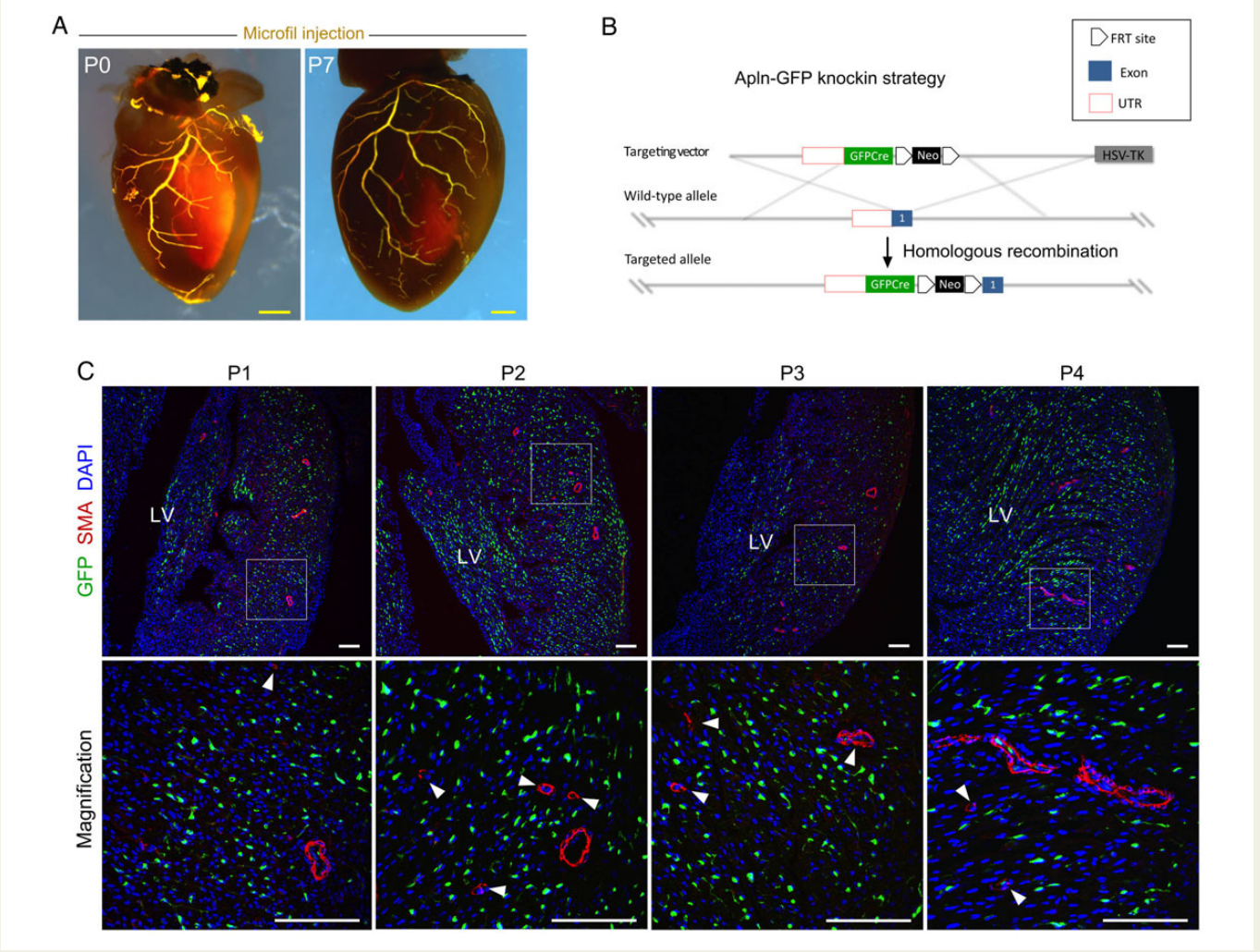

Figure 1 APLN expression in neonatal hearts. (*A*) Microfil injection into the coronary vascular circulation at P0 and P7 highlights the established, patent coronary vasculature. (*B*) A schematic model shows the knock-in strategy for generating the Apln-GFP allele by homologous recombination. (*C*) APLN expression was studied by analysis of post-natal day 1 (P1)–P4 neonatal hearts. Immunostaining for GFP as surrogate of APLN, SMA, and DAPI on sections of embryonic or neonatal Apln-GFP hearts revealed that Apln is expressed in capillaries, but is significantly reduced in large and small size arteries. Boxed regions are ventricle free wall and are magnified in figures in the lower panels. Arrowheads indicate APLN^{-}SMA^{+} coronary arteries. Each image is a representative of three to four individual samples. Scale bars: yellow, 0.5 mm; white, 100 μm.

of Apln (*Figure 1B*). Immunostaining for GFP (as a surrogate for Apln expression) and SMA (for SMCs) on sections from Apln-GFP neonatal hearts showed that Apln is robustly expressed in capillary vessels, but sparsely expressed in large and small diameter arterial vessel endothelial cells (*Figure 1C*). By analysing neonatal hearts from Apln-LacZ and Apln-CreER knock-in mouse lines in conjunction with either X-gal staining or estrogen receptor (ESR) immunostaining, respectively, we also detected elevated Apln expression in capillary endothelial cells, but reduced Apln expression in arterial endothelial cells (Supplementary material online, *Figure S2*). Accordingly, we focused our attention on the two different types of vessels (arteries and capillaries) present in the post-natal heart and examined coronary vessel development and collateral vessel formation during coronary regeneration.

3.2 Labelling of coronary capillary and arterial endothelial cells by Apln-CreER

We next performed genetic lineage tracing analysis using Cre-loxP reporter mice and an Apln-CreER driver to determine whether the differential expression of Apln in the neonatal heart could be used to genetically distinguish these two types of vascular endothelial cells (capillary and artery) (*Figure 2A*). Genetic labelling based on Cre-LoxP-mediated recombination is permanent and heritable,[41] so that the descendants of Apln-CreER-labelled cells always express the recombined reporter, even if they do not actively express Apln. We adopted two different strategies using early embryonic (E10.5) or neonatal (P1) administration of tamoxifen to label the post-natal coronary vessels (*Figure 2B*). By examining the outer myocardial wall, we found that tamoxifen induction at E10.5 labelled the major coronary arteries, as well as the coronary capillaries of post-natal day (P7) hearts (*Figure 2C*, E10.5 Tam. group). During embryogenesis, the coronary artery stems arise from peritruncal capillary beds and subsequently connect to the aorta. This embryonic process represents the *de novo* formation of the coronary artery stem, rather than growth directly from the existing aorta.[10,42,43] The coronary artery matures through subsequent vascular remodelling of the Apln-CreER-labelled capillary plexus and the subsequent recruitment of pericytes and SMCs (*Figure 2C*, E10.5 Tam. group). In contrast, tamoxifen treatment at P1 sparsely labelled arterial endothelial cells (*Figure 2C*, P1 Tam. group). This result makes sense in light of the fact that coronary arteries in the neonatal heart do not

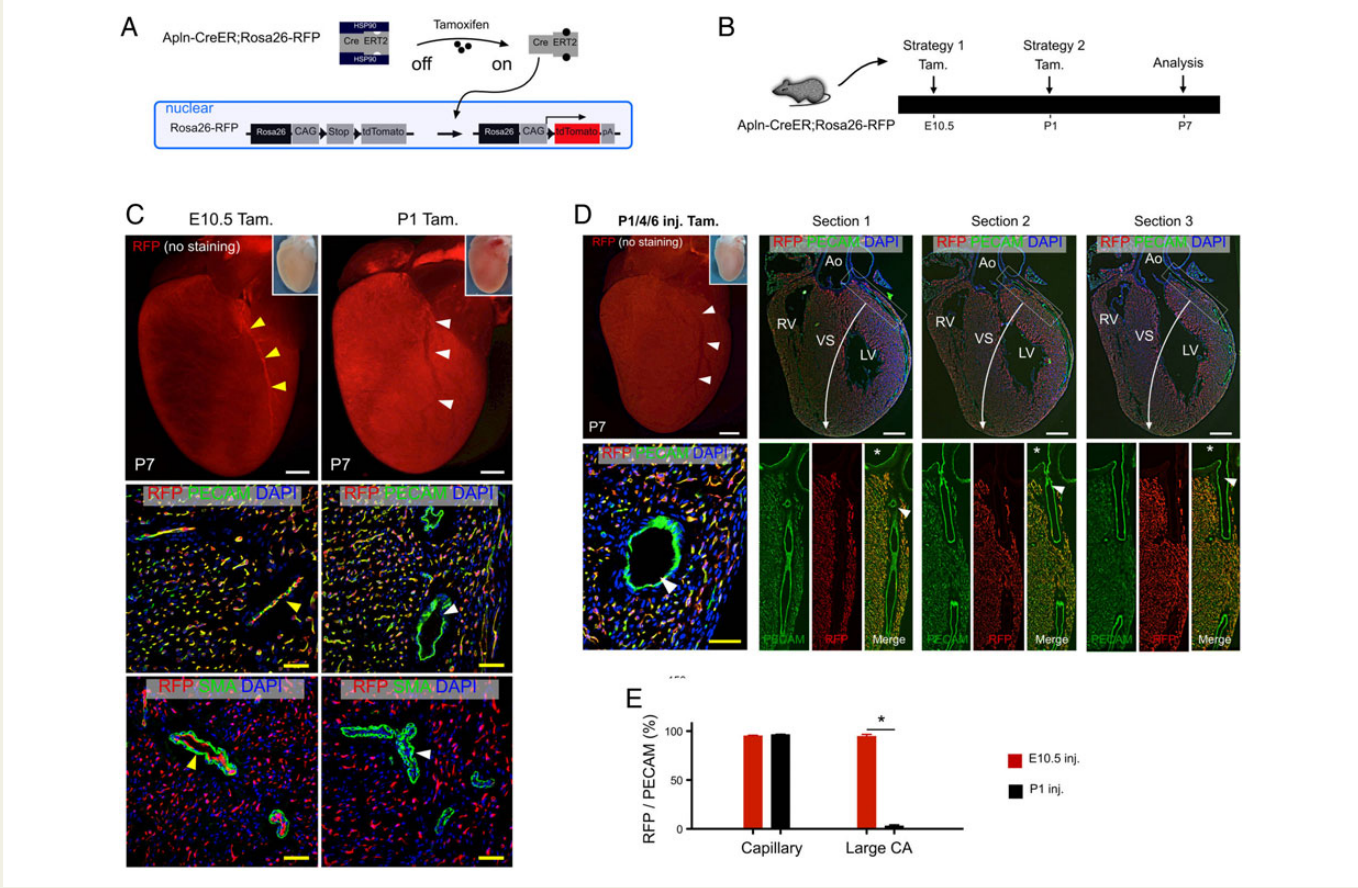

Figure 2 Labelling of coronary capillaries and arteries by Apln-CreER. (*A*) A schematic figure showing tamoxifen induction of CreER activity and genetic labelling of Apln^{+} cells. (*B*) Strategies for tamoxifen induction (Tam.) and analysis of coronary artery labelling in Apln-CreER; Rosa26-RFP mice. (*C*) Whole-mount view (top) and stained sections (below) of P7 Apln-CreER; Rosa26-RFP hearts following tamoxifen treatment. Tamoxifen induction at E10.5, but not P1, labels endothelial cells (PECAM+) of major coronary arteries (yellow vs. white arrowheads). (*D*) Whole-mount view and serial sections (50 μm apart, sections progress left to right from ventral to dorsal panels) of P7 Apln-CreER; Rosa26-RFP hearts following serial neonatal tamoxifen induction (P1/4/6). The endothelium of the coronary arteries is sparsely labelled (white arrowheads). Asterisks indicate orifices in the aorta. (*E*) Quantification of RFP^{+}PECAM^{+} cells of the capillaries and large coronary arteries in the outer myocardial wall of P7 hearts following tamoxifen induction at E10.5 or P1. *$P < 0.05$, $n = 5–6$ per group. LV, left ventricle; RV, right ventricle; VS, ventricular septum; Ao, aorta. Scale bars: white bar, 0.5 mm; yellow bar, 50 μm.

actively express Apln at the time of tamoxifen treatment (P1, *Figure 1C*). To exclude the possibility that the differences observed in Apln-CreER-mediated coronary artery labelling were due to differential efficiency of CreER-mediated recombination at the two different induction time points, we performed serial tamoxifen injections (P1, P4, and P6) to ensure that tamoxifen was not rate-limiting and to allow for maximal CreER activity. Consistently, we found that the large coronary arteries were infrequently labelled by Apln-CreER after P1, whereas the vast majority of capillary endothelial cells were labelled (*Figure 2D* and *E*). Collectively, these results established a strategy that could genetically distinguish capillary endothelial cells from large diameter arterial endothelial cells.

3.3 Genetic lineage tracing reveals collateral vessel formation after neonatal MI

The differential pattern of Apln expression and CreER activity provided us with a novel approach to visualize the contribution of capillaries and arteries to collateral artery formation. Our previous work showed that Apln is not robustly expressed in the post-natal heart prior to MI, making it difficult to label the capillaries in a non-ischaemic, healthy heart. To induce efficient labelling of capillaries and to stimulate robust coronary collateral vessel formation, we established a neonatal MI model by ligating the LAD coronary artery in the P4 neonatal mouse heart.[28] TTC staining verified that our neonatal MI injury model was successful (*Figure 3A*). This early neonatal injury model provides a myocardial

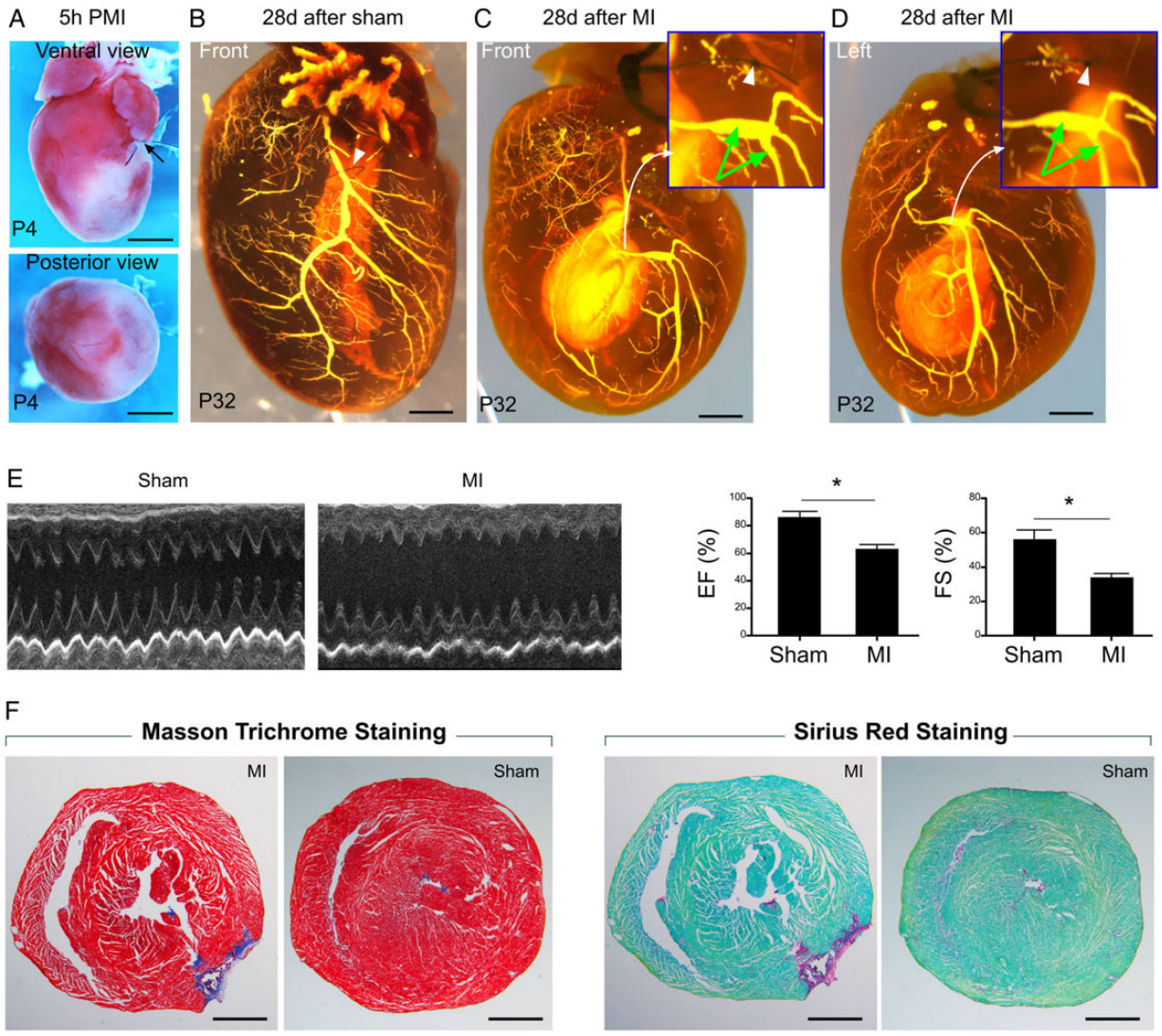

Figure 3 Establishment of a neonatal MI injury model. (*A*) TTC (2,3,5-triphenyltetrazolium chloride) staining of P4 hearts demarcates damaged myocardium (infarct zone) after ligation of the LAD coronary artery (black arrow). (*B*) Microfil-injected heart 28 days (28d) after sham surgery. White arrowhead points to the non-ligated coronary artery. (*C* and *D*) Ventral and left-sided views of microfil-injected heart 28 days after MI. White arrowheads indicate the ligation site of the previous LAD coronary artery. Green arrows indicate newly established major coronary arteries that bypass the ligation point. $n = 3–4$. Scale bars: 1 mm. (*E*) Functional measurement of MI hearts by M-mode echocardiography showing systolic and diastolic cardiac contractions. Two indicators of cardiac output, EF and FS, calculated from the echocardiography, were markedly reduced in MI hearts when compared with sham-operated controls. $n = 4$. (*F*) Masson's trichrome and Sirius Red staining of MI and control hearts. MI was performed on P4 neonatal hearts by ligation of the LAD artery, and hearts were collected 28 days after MI (at P32). Significant fibrosis was induced in the left apex of the ventricle, indicating effective MI induction. All the mice used here are wild-type ICR/C57BL6/J-mixed background mice. $n = 4$. Black bars, 1 mm.

insult that is overcome by partial cardiac regeneration and robust collateral vessel formation. Hearts were collected 28 days (at P32) after MI (at P4), and the patent coronary arterial network was visualized in both sham-operated and MI hearts (*Figure 3B–D*). We found that the coronary arterial network is re-established by large size collateral arteries bypassing the ligation site (*Figure 3C* and *D*). Functional and histological assessment of the post-MI hearts revealed reduced cardiac function (*Figure 3E*) and extensive fibrosis compared with sham-operated controls (*Figure 3F*). Collectively, these data verify the utility of a neonatal MI model for inducing collateral vessel formation in mice.

To determine whether the new large collateral vessels formed from a pre-existing artery or capillary endothelial cells, we induced Apln-CreER labelling of the early capillaries at P1 prior to MI (*Figure 4A*). Following injury, the newly formed large diameter coronary arteries (collateral vessels) surrounding the ligation site were infrequently labelled by neonatal Apln-CreER activity (RFP^-; $PECAM^+$), whereas the capillaries were robustly labelled (RFP^+; $PECAM^+$) (*Figure 4A* and *B*). These data demonstrated that the new large diameter collateral vessels formed in response to MI were not derived primarily from the capillary vessels. Instead, it is likely that these RFP^- large diameter collateral vessels are formed from pre-existing arteries, which were not efficiently labelled by neonatal Apln-CreER activity. Altogether, these results suggest that arteriogenesis, rather than arterialization, was the primary mechanism underlying collateral vessel formation in the injured neonatal heart.

To definitely determine whether large collateral arteries are indeed derived from pre-existing arteries, we took advantage of the fact that tamoxifen induction at E10.5 labelled most arterial endothelial cells in the post-natal heart (*Figure 5A* and *B*). Significantly, tamoxifen induction at E10.5 also efficiently labelled the large collateral vessels of the P32 heart (*Figure 5C* and *D*), indicating that these collateral vessels are formed from pre-existing coronary arteries present at P4. Collectively, these data indicate that arteriogenesis, but not arterialization, is the main mechanism responsible for the formation of the large diameter collateral vessel in the post-natal heart.

3.4 Labelling of small diameter coronary arteries after neonatal injury

Apln expression is significantly reduced in small diameter coronary arteries when compared with capillaries in the neonatal heart (*Figure 1C*). However, the neonatal heart is still undergoing development and remodelling, and a substantial number of coronary vessels (especially capillaries) arise *de novo* during this stage.[40] These newly formed capillaries could generate small size arteries during post-natal development. To test this, we injected tamoxifen at P1 and analysed hearts at both P4 and P32 to determine whether small arteries were labelled (*Figure 6A*). We found that induction of Apln-CreER activity at P1 led to infrequent labelling of small coronary arteries (when compared with capillaries) at P4. However, the labelling of small arteries increased significantly by P32 (*Figure 6B* and *C*), suggesting that capillaries remodel and mature into small arteries during the first month of post-natal development and growth. Because small arteries could be formed *de novo* during neonatal heart development, our genetic lineage tracing of neonatal coronary vessels cannot delineate whether small diameter collateral arteries are formed after neonatal heart injury.

3.5 Large and small size coronary arteries are derived from pre-existing arteries during adult MI

Given the results of our neonatal studies, we wondered whether a similar mechanism regulated collateral vessel growth in a more physiologically relevant model. Accordingly, we employed an adult MI model to study whether any collateral arteries could form from pre-existing arteries, as arteries are already present and stable in the adult heart prior to MI (unlike the concomitant growth and remodelling of vessels occurring in the neonatal MI model). Our previous work showed that most coronary vessels are quiescent during homeostasis, with expression of Apln detectable following MI.[22] To efficiently label these coronary vessels, we administered tamoxifen induction to Apln-CreER; Rosa26-RFP

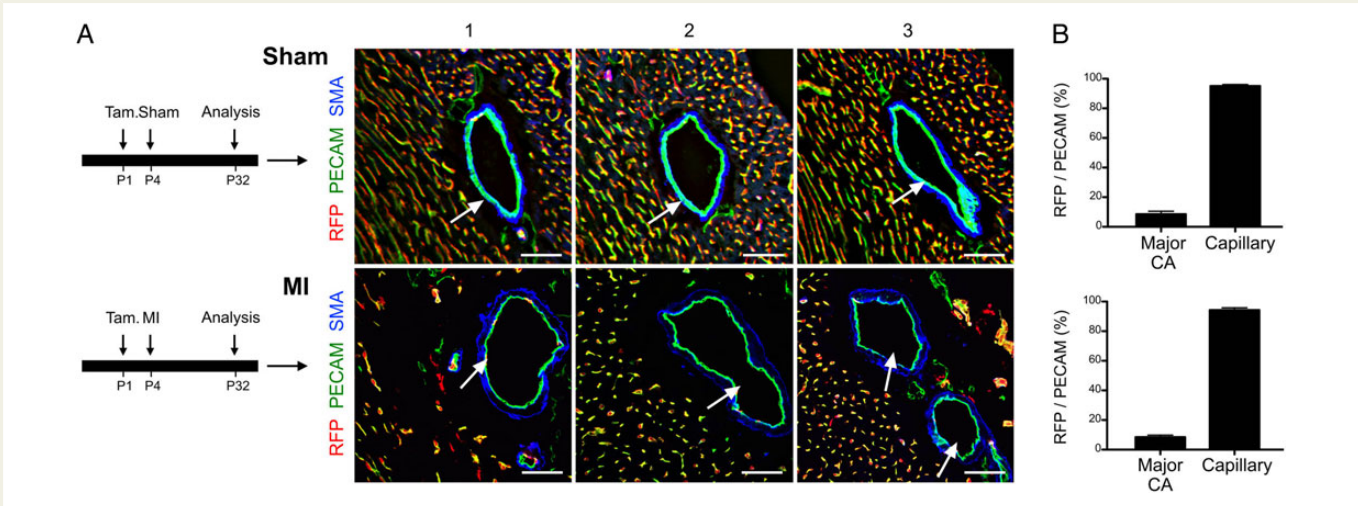

Figure 4 Fate map of arteries and capillaries following MI. (*A*) The experimental timeline for tamoxifen induction of Apln-CreER activity in the post-natal heart after sham or surgery. Immunostaining for RFP, PECAM, and SMA on sections of P32 Apln-CreER; Rosa26-RFP hearts after tamoxifen treatment (Tam.) at P1. White arrows point to the collateral arteries, which were not significantly labelled in either sham or MI hearts, suggesting that these major large diameter adult coronary arteries are not formed *de novo* from labelled capillaries at P1. (*B*) The extent of labelling is quantified as the percentage of RFP+ endothelial cells over total $PECAM^+$ endothelial cells. There is significant difference between major coronary artery and capillaries in RFP^+ cell percentage ($P < 0.05$, $n = 3–4$). Scale bars: 50 μm.

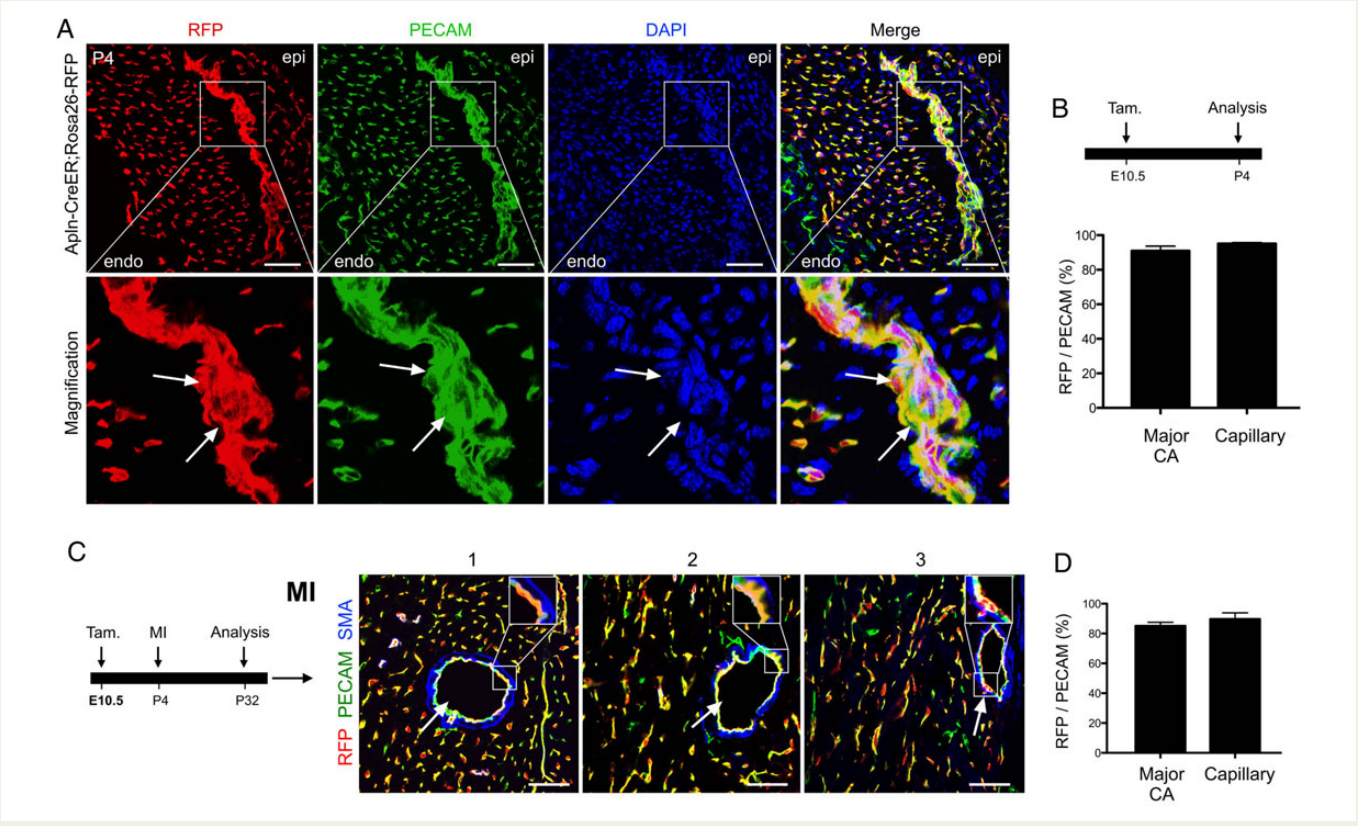

Figure 5 Robust labelling of large coronary arteries following E10.5 tamoxifen treatment. (*A*) Immunostaining for RFP and PECAM on sections from Apln-CreER; Rosa26-RFP hearts showed robust labelling of arterial endothelial cells (RFP$^+$, white arrows), as well as capillaries. Epi, epicardium; endo, endocardium. (*B*) The experimental strategy is shown above. Below, quantification of the labelling efficiency is shown. Labelling efficiency was calculated as the percentage of RFP$^+$ cells in PECAM$^+$ vessels of the outer myocardial wall. Scale bars, 100 μm. (*C*) Immunostaining for RFP and PECAM showed that collateral arterial endothelial cells (white arrows) were labelled in the MI hearts. Tamoxifen was administered at E10.5. Scale bars, 50 μm. (*D*) Quantification of the percentage of RFP+ endothelial cells. Each image is representative of three individual samples.

mice at 2 days (D2) after MI (achieved by permanent ligation of the LAD coronary artery) and collected hearts at D4 and D30 for determination of vessel labelling (*Figure 7A*). We found that Apln-CreER significantly labels tissues of the infarct and border zones at D4 after ligation (*Figure 7B*). Immunostaining for RFP and SMA on sections from D4 hearts revealed that most coronary capillaries are RFP$^+$, whereas both the small and large coronary arteries are not significantly labelled by Apln-CreER activity (*Figure 7C*). Analysis of D30 hearts also revealed significant labelling in the left ventricle infarct and border zones (*Figure 7D*). We found that few coronary arteries are labelled in the border zone of the left ventricle (*Figure 7E*). Immunostaining for RFP, SMA, and VE-Cadherin (VE-CAD; Cdh5) showed that most coronary arteries (both small and large) are not RFP$^+$ (*Figure 7F*), suggesting that they are not derived through arterialization. Currently, some studies suggest that endothelial cell growth from pre-existing collaterals is driven by shear stress, rather than hypoxia (a known inducer of Apln).[44,45] Thus, we employed an *in vitro* endothelial cell shear stress model to determine whether shear stress is sufficient to induce Apln expression. We found that shear stress failed to increase Apln transcript levels in cultured human endothelial cells (Supplementary material online, *Figure S3*). Taken together, these results demonstrate that the remaining coronary arteries in the border and infarct zones are derived from pre-existing coronary arteries, rather than forming *de novo* from capillaries through arterialization, supporting arteriogenesis as the major mechanism of collateral vessel formation in the adult heart.

4. Discussion

During development, arteries are initially formed *de novo* through the coalescence and remodelling of a preliminary capillary network, and the subsequent recruitment of pericytes and SMCs generates a stable, patent coronary network. Whether this same developmental process was redeployed in an injury setting remained unknown. Previous studies in ischaemic models suggested that collateral arteries primarily derive from pre-existing arteriolar connections through arteriogenesis.[1,46] However, arterialization could also account for at least some of the collateral vessels detected by angiography, and at a minimum, this mechanism for collateral vessel growth could not be excluded.[13] A primary reason for the lack of a definitive answer regarding the extent of either mechanism's involvement in collateral vessel growth is due to the absence of tools that distinguish between the capillary endothelium and pre-existing arterial endothelial cells *in vivo*.[2] Indeed, arterialization and arteriogenesis have different molecular, cellular, and anatomical mechanisms. Arterialization involves hypoxia-induced angiogenesis and the recruitment of new SMCs to an ischaemic region, whereas arteriogenesis is largely influenced by haemodynamic stimuli, such as fluid

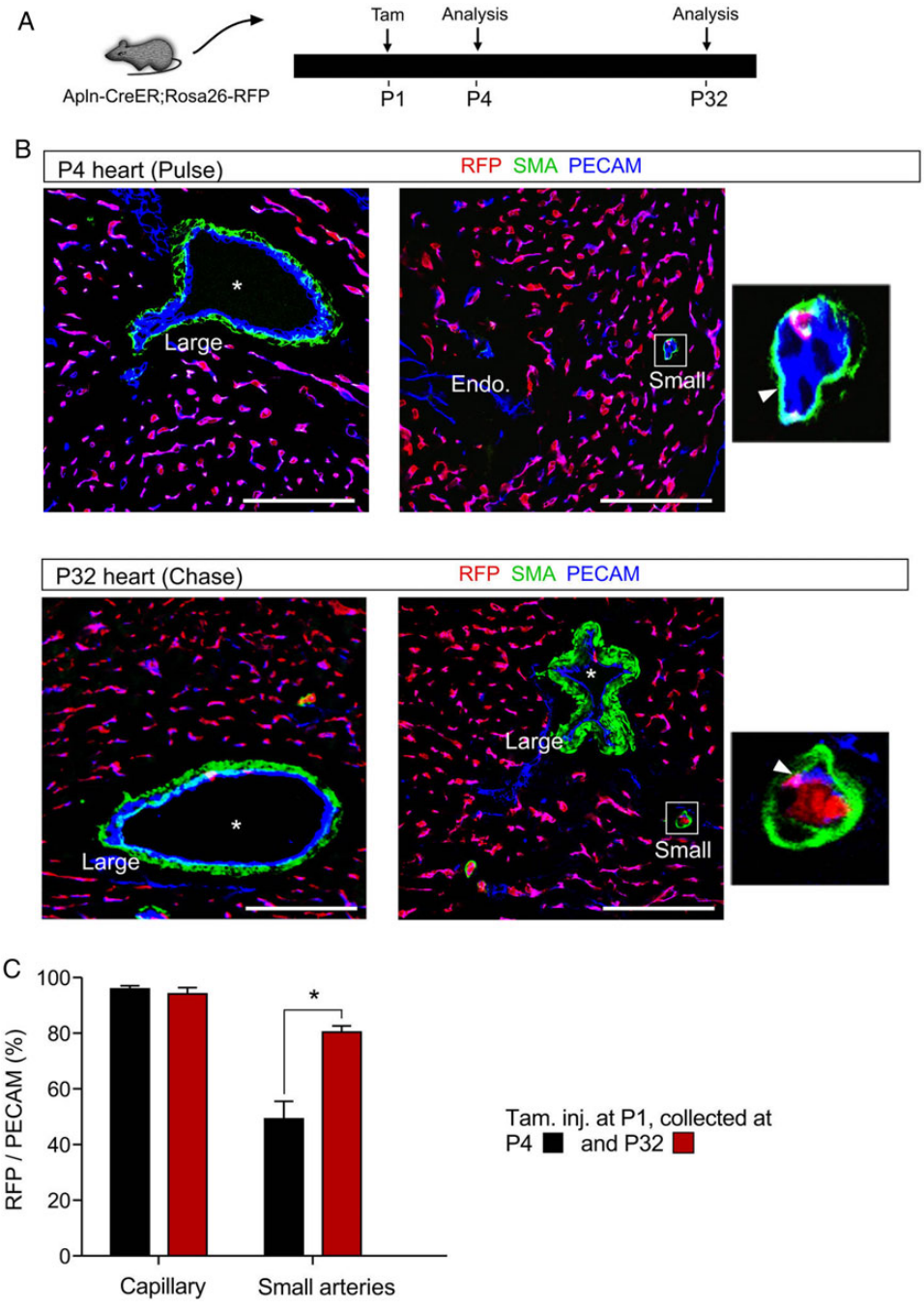

Figure 6 Labelling of small coronary arteries in the neonatal and adult heart. (*A*) A schematic figure shows the strategy for tamoxifen induction (Tam) and analysis (at P4 and P32). (*B*) Immunostaining for RFP, SMA, and PECAM on sections of P4 Apln-CreER; Rosa26-RFP hearts after Tamoxifen treatment at P1. Arrowheads indicate a small size artery (<30 μm); asterisks indicate large artery (>60 μm); Endo, endocardium. Scale bars, 100 μm. (*C*) Quantification of labelling efficiency, defined as the percentage of $RFP^{+}PECAM^{+}$ endothelial cells compared with total $PECAM^{+}$ vascular endothelial cells. Student's *t*-test was used to analyse differences, and values are shown as mean ± SEM; $^{*}P < 0.05$; $n = 3–4$.

shear stress, that activate an "outward remodelling" programme within the vessel wall.[44,45] One additional difference between these two mechanisms is the vessel bed that actually contributes endothelial cells to the collateral arteries. Whereas arteriogenesis emphasizes the contribution of endothelial cells from pre-existing arteries, the arterialization model posits that a new artery arises from the capillary endothelium.

The ultimate fate of these endothelial cells, regardless of their initial source, will be a patent artery for the conduction of coronary blood flow to allow for increased perfusion of the cardiac tissue. Our lineage tracing results, prompted by the differential expression of Apln in the arterial and capillary endothelium, revealed genetically that arteriogenesis is the dominant mechanism for the formation of the large size collateral arteries during neonatal MI. The formation of large collateral arteries may still be predominantly influenced by haemodynamics and shear stress.[2,45] We also noticed in the neonatal heart that the difference of Apln expression between small artery and capillary

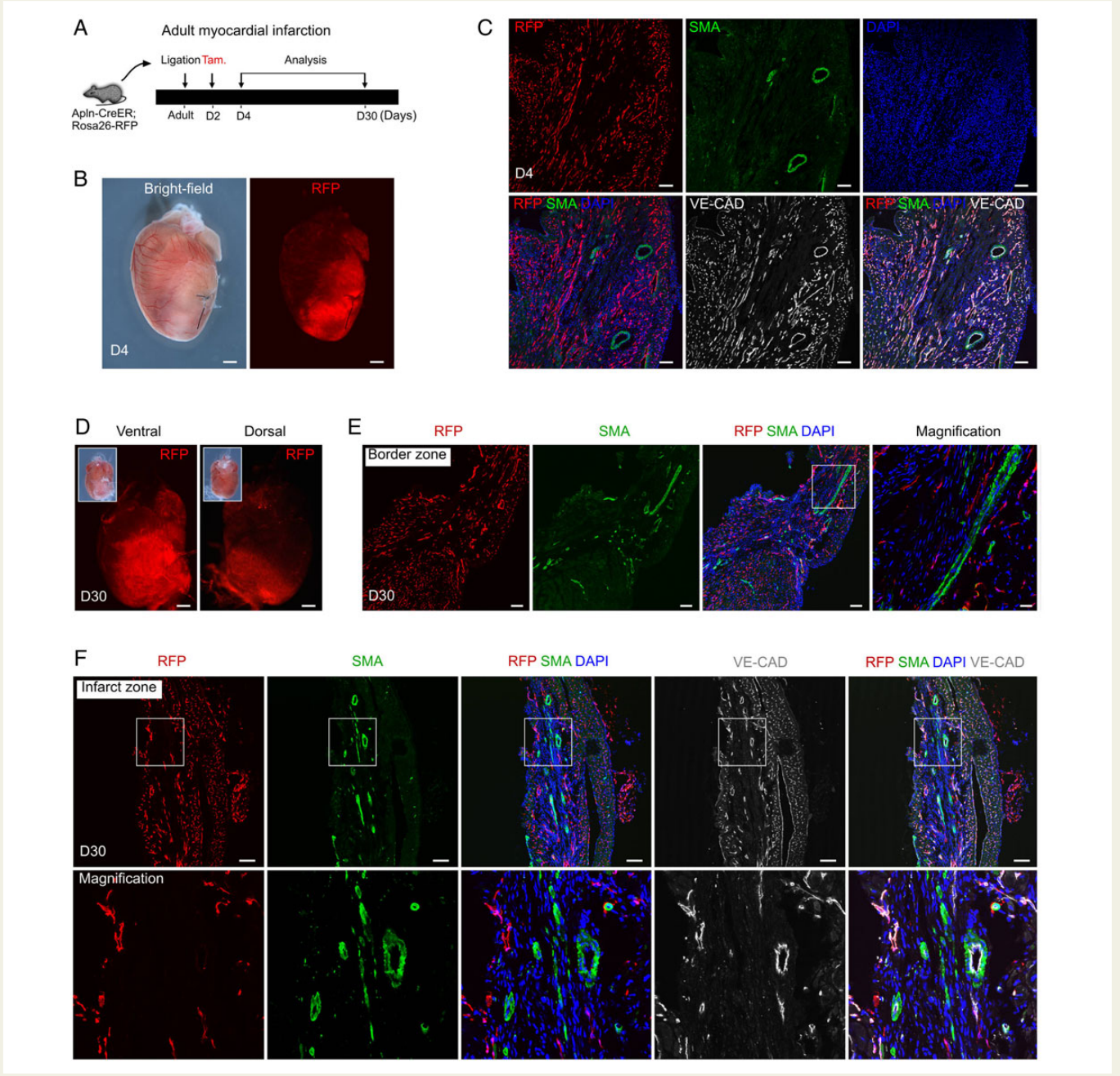

Figure 7 Coronary arteries in the infarcted myocardium are derived from pre-existing arteries but not from capillaries. (*A*) Schematic showing the experimental strategy for injury, tamoxifen induction, and analysis. (*B*) Whole-mount bright-field and fluorescent views of Apln-CreER; Rosa26-RFP hearts at day 4 (D4) after MI. (*C*) Immunostaining for RFP, SMA, and VE-CAD showed that Apln-CreER robustly labels VE-CAD^{+}SMA^{-} coronary capillaries, but not VE-CAD+SMA+ coronary arteries. (*D*) Whole-mount view of Apln-CreER; Rosa26-RFP hearts at D30 after MI. Insets are bright-field views of hearts. (*E*) Immunostaining for RFP and SMA showed that Apln-CreER-labelled capillaries do not form coronary arteries in the border zone. (*F*) Immunostaining for RFP, SMA, and VE-CAD showed that Apln-CreER-labelled coronary capillaries do not contribute significantly to coronary arteries in the infarct zone. Scale bars: 1 mm in (*B*) and (*D*) and 100 μm in (*C*), (*E*), and (*F*). Each image is representative of three individual samples.

endothelial cells is not as significant as that between large artery and capillary endothelial cells (*Figures 6C* and *2E*). More importantly, the neonatal heart is still undergoing development and remodelling, and new coronary vessels are actively forming in this model. Accordingly, from P4 to P32, we could detect an increase in small arteries that are formed *de novo* (*Figure 6C*) during normal development. This prevented us from determining whether small size collateral arteries are actively formed following injury in the neonatal heart. It is possible that some small size collateral arteries, especially those downstream of the ischaemic region of the ligation site, may form *de novo* via arterialization following MI in the neonatal heart.

In the injured region distal to the ligation site, which is significantly ischaemic,[2] increased angiogenesis and remodelling (arterialization) might take place in response to coronary artery ligation. To directly address this possibility, we performed lineage tracing studies in an adult mouse MI model. Our results demonstrated that the remaining

coronary arteries in both the border and the infarct zones are derived from pre-existing coronary arteries, but not from Apln-CreER^{+} capillaries. These adult lineage tracing data suggested that the majority of large and small size collateral arteries are formed by arteriogenesis, rather than through arterialization, following MI in the adult heart.

Herein, we identify Apln-CreER as a novel tool that distinguishes coronary artery and capillary endothelial cells. Through monitoring Apln expression and performing genetic lineage tracing experiments using Apln-CreER, in conjunction with an MI injury model, we show that arteriogenesis is the major mechanism accounting for collateral artery formation during MI.

Supplementary material

Supplementary Material is available at *Cardiovascular Research* online.

Acknowledgements

We thank Thomas Quertermous for providing the Apln-LacZ line and Hongkui Zeng for providing the Rosa26-RFP mice. We thank Shanghai Biomodel Organism Co., Ltd for generating the Apln-GFP knock-in mouse line.

Conflict of interest: none declared.

Funding

This work was supported by National Science Foundation of China (91339104, 31271552, 31222038, 31301188, 31571503, and 31501172), Ministry of Science and Technology (2012CB945102 and 2013CB945302), Shanghai Zhangjiang Stem Cell Research Project (ZJ2014-ZD-002), Shanghai Basic Research Key Project (14JC1407400), China Postdoctoral Science Foundation (2013M541561, 2015M570389, and 2015M581669), Youth Innovation Promotion Association of Chinese Academy of Sciences (2015218), Shanghai Yangfan Project (15YF1414000), Shanghai Rising-Star Program (15QA1404300), Shanghai Institutes for Biological Sciences (SIBS) President Fund, and SIBS Postdoc Fund (2013KIP311 and 2014KIP314), Sanofi-SIBS Fellowship and AstraZeneca. J.D.W. was supported by a Scientist Development Grant from the American Heart Association (12SDG12060353) and seed funds from the Cardiovascular Research Institute at Baylor College of Medicine. Funding to pay the Open Access publication charges for this article was provided by. . .

References

1. Helisch A, Schaper W. Arteriogenesis: the development and growth of collateral arteries. *Microcirculation* 2003;**10**:83–97.
2. Rubanyi GM. Mechanistic, technical, and clinical perspectives in therapeutic stimulation of coronary collateral development by angiogenic growth factors. *Mol Ther* 2013;**21**:725–738.
3. Ito W, Arras M, Winkler B, Scholz D, Schaper J, Schaper W. Monocyte chemotactic protein-1 increases collateral and peripheral conductance after femoral artery occlusion. *Circ Res* 1997;**80**:829–837.
4. Arras M, Ito W, Scholz D, Winkler B, Schaper J, Schaper W. Monocyte activation in angiogenesis and collateral growth in the rabbit hindlimb. *J Clin Invest* 1998;**101**:40–50.
5. Belmadani S, Matrougui K, Kolz C, Pung YF, Palen D, Prockop DJ, Chilian WM. Amplification of coronary arteriogenic capacity of multipotent stromal cells by epidermal growth factor. *Arterioscler Thromb Vasc Biol* 2009;**29**:802–808.
6. Rocic P, Kolz C, Reed R, Potter B, Chilian WM. Optimal reactive oxygen species concentration and p38 map kinase are required for coronary collateral growth. *Am J Physiol Heart Circ Physiol* 2007;**292**:H2729–H2736.
7. Berk B, Fujiwara K, Lehoux S. ECM remodeling in hypertensive heart disease. *J Clin Invest* 2007;**117**:568–575.
8. White FC, Bloor CM, McKirnan MD, Carroll SM. Exercise training in swine promotes growth of arteriolar bed and capillary angiogenesis in heart. *J Appl Physiol* 1998;**85**:1160–1168.
9. Faber JE, Chilian WM, Deindl E, van Royen N, Simons M. A brief etymology of the collateral circulation. *Arterioscler Thromb Vasc Biol* 2014;**34**:1854–1859.
10. Tian X, Hu T, He L, Zhang H, Huang X, Poelmann RE, Liu W, Yang Z, Yan Y, Pu WT, Zhou B. Peritruncal coronary endothelial cells contribute to proximal coronary artery stems and their aortic orifices in the mouse heart. *PLoS ONE* 2013;**8**:e80857.
11. Deindl E, Buschmann I, Hoefer IE, Podzuweit T, Boengler K, Vogel S, van Royen N, Fernandez B, Schaper W. Role of ischemia and of hypoxia-inducible genes in arteriogenesis after femoral artery occlusion in the rabbit. *Circ Res* 2001;**89**:779–786.
12. Schaper W, Ito W. Molecular mechanisms of coronary collateral vessel growth. *Circ Res* 1996;**79**:911–919.
13. Hershey JC, Baskin EP, Glass JD, Hartman HA, Gilberto DB, Rogers IT, Cook JJ. Revascularization in the rabbit hindlimb: dissociation between capillary sprouting and arteriogenesis. *Cardiovasc Res* 2001;**49**:618–625.
14. Charo D, Ho M, Fajardo G, Kawana M, Kundu R, Sheikh A, Finsterbach T, Leeper N, Ernst K, Chen M, Ho Y, Chun H, Bernstein D, Ashley E, Quertermous T. Endogenous regulation of cardiovascular function by apelin-apj. *Am J Physiol Heart Circ Physiol* 2009;**297**:H1904–H1913.
15. Kleinz M, Skepper J, Davenport A. Immunocytochemical localisation of the apelin receptor, apj, to human cardiomyocytes, vascular smooth muscle and endothelial cells. *Regul Pept* 2005;**126**:233–240.
16. Kuba K, Zhang L, Imai Y, Arab S, Chen M, Maekawa Y, Leschnik M, Leibbrandt A, Markovic M, Schwaighofer J, Beetz N, Musialek R, Neely G, Komnenovic V, Kolm U, Metzler B, Ricci R, Hara H, Meixner A, Nghiem M, Chen X, Dawood F, Wong K, Sarao R, Cukerman E, Kimura A, Hein L, Thalhammer J, Liu P, Penninger J. Impaired heart contractility in apelin gene-deficient mice associated with aging and pressure overload. *Circ Res* 2007;**101**:e32–e42.
17. Eyries M, Siegfried G, Ciumas M, Montagne K, Agrapart M, Lebrin F, Soubrier F. Hypoxia-induced apelin expression regulates endothelial cell proliferation and regenerative angiogenesis. *Circ Res* 2008;**103**:432–440.
18. Ronkainen V, Ronkainen J, Hanninen S, Leskinen H, Ruas J, Pereira T, Poellinger L, Vuolteenaho O, Tavi P. Hypoxia inducible factor regulates the cardiac expression and secretion of apelin. *FASEB J* 2007;**21**:1821–1830.
19. Kalin R, Kretz M, Meyer A, Kispert A, Heppner F, Brandli A. Paracrine and autocrine mechanisms of apelin signaling govern embryonic and tumor angiogenesis. *Dev Biol* 2007;**305**:599–614.
20. Yu Q, Hirst C, Costa M, Ng E, Schiesser J, Gertow K, Stanley E, Elefanty A. Apelin promotes hematopoiesis from human embryonic stem cells. *Blood* 2012;**119**:6243–6254.
21. Tempel D, de Boer M, van Deel E, Haasdijk R, Duncker D, Cheng C, Schulte-Merker S, Duckers H. Apelin enhances cardiac neovascularization after myocardial infarction by recruiting aplnr+ circulating cells. *Circ Res* 2012;**111**:585–598.
22. Liu Q, Hu T, He L, Huang X, Tian X, Zhang H, He L, Pu W, Zhang L, Sun H, Fang J, Yu Y, Duan S, Hu C, Hui L, Zhang H, Quertermous T, Xu Q, Red-Horse K, Wythe JD, Zhou B. Genetic targeting of sprouting angiogenesis using apln-creer. *Nat Commun* 2015;**6**:6020.
23. Liu P, Jenkins N, Copeland N. A highly efficient recombineering-based method for generating conditional knockout mutations. *Genome Res* 2003;**13**:476–484.
24. Tian X, Hu T, Zhang H, He L, Huang X, Liu Q, Yu W, He L, Yang Z, Zhang Z, Zhong T, Yang X, Yang Z, Yan Y, Baldini A, Sun Y, Lu J, Schwartz R, Evans S, Gittenberger-de Groot A, Red-Horse K, Zhou B. Subepicardial endothelial cells invade the embryonic ventricle wall to form coronary arteries. *Cell Res* 2013;**23**:1075–1090.
25. Sheikh A, Chun H, Glassford A, Kundu R, Kutschka I, Ardigo D, Hendry S, Wagner R, Chen M, Ali Z, Yue P, Huynh D, Connolly A, Pelletier M, Tsao P, Robbins R, Quertermous T. *In vivo* genetic profiling and cellular localization of apelin reveals a hypoxia-sensitive, endothelial-centered pathway activated in ischemic heart failure. *Am J Physiol Heart Circ Physiol* 2008;**294**:H88–H98.
26. Madisen L, Zwingman T, Sunkin S, Oh S, Zariwala H, Gu H, Ng L, Palmiter R, Hawrylycz M, Jones A, Lein E, Zeng H. A robust and high-throughput cre reporting and characterization system for the whole mouse brain. *Nat Neurosci* 2010;**13**:133–140.
27. Miquerol L, Beyer S, Kelly R. Establishment of the mouse ventricular conduction system. *Cardiovasc Res* 2011;**91**:232–242.
28. Xin M, Kim Y, Sutherland L, Murakami M, Qi X, McAnally J, Porrello E, Mahmoud A, Tan W, Shelton J, Richardson J, Sadek H, Bassel-Duby R, Olson E. Hippo pathway effector yap promotes cardiac regeneration. *Proc Natl Acad Sci USA* 2013;**110**:13839–13844.
29. He L, Tian X, Zhang H, Wythe J, Zhou B. Fabp4-creer lineage tracing reveals two distinctive coronary vascular populations. *J Cell Mol Med* 2014;**18**:2152–2156.
30. Zhou B, Honor L, He H, Ma Q, Oh J, Butterfield C, Lin R, Melero-Martin J, Dolmatova E, Duffy H, Gise A, Zhou P, Hu Y, Wang G, Zhang B, Wang L, Hall J, Moses M, McGowan F, Pu W. Adult mouse epicardium modulates myocardial injury by secreting paracrine factors. *J Clin Invest* 2011;**121**:1894–1904.
31. Tian X, Pu WT, Zhou B. Cellular origin and developmental program of coronary angiogenesis. *Circ Res* 2015;**116**:515–530.
32. Gerber H, Hillan K, Ryan A, Kowalski J, Keller G, Rangell L, Wright B, Radtke F, Aguet M, Ferrara N. Vegf is required for growth and survival in neonatal mice. *Development* 1999;**126**:1149–1159.
33. Kisanuki Y, Hammer R, Miyazaki J, Williams S, Richardson J, Yanagisawa M. Tie2-cre transgenic mice: a new model for endothelial cell-lineage analysis *in vivo*. *Dev Biol* 2001;**230**:230–242.

34. Alva J, Zovein A, Monvoisin A, Murphy T, Salazar A, Harvey N, Carmeliet P, Iruela-Arispe M. Ve-cadherin-cre-recombinase transgenic mouse: a tool for lineage analysis and gene deletion in endothelial cells. *Dev Dyn* 2006;**235**:759–767.
35. Monvoisin A, Alva J, Hofmann J, Zovein A, Lane T, Iruela-Arispe M. Ve-cadherin-creert2 transgenic mouse: a model for inducible recombination in the endothelium. *Dev Dyn* 2006;**235**:3413–3422.
36. Lee S, Chen T, Barber C, Jordan M, Murdock J, Desai S, Ferrara N, Nagy A, Roos K, Iruela-Arispe M. Autocrine vegf signaling is required for vascular homeostasis. *Cell* 2007;**130**:691–703.
37. Wang Y, Nakayama M, Pitulescu M, Schmidt T, Bochenek M, Sakakibara A, Adams S, Davy A, Deutsch U, Luthi U, Barberis A, Benjamin L, Makinen T, Nobes C, Adams R. Ephrin-b2 controls vegf-induced angiogenesis and lymphangiogenesis. *Nature* 2010; **465**:483–486.
38. Gustafsson E, Brakebusch C, Hietanen K, Fassler R. Tie-1-directed expression of cre recombinase in endothelial cells of embryoid bodies and transgenic mice. *J Cell Sci* 2001;**114**:671–676.
39. Red-Horse K, Ueno H, Weissman I, Krasnow M. Coronary arteries form by developmental reprogramming of venous cells. *Nature* 2010;**464**:549–553.
40. Tian X, Hu T, Zhang H, He L, Huang X, Liu Q, Yu W, He L, Yang Z, Yan Y, Yang X, Zhong TP, Pu WT, Zhou B. *De novo* formation of a distinct coronary vascular population in neonatal heart. *Science* 2014;**345**:90–94.
41. Kretzschmar K, Watt F. Lineage tracing. *Cell* 2012;**148**:33–45.
42. Bogers A, Gittenberger-de Groot A, Dubbeldam J, Huysmans H. The inadequacy of existing theories on development of the proximal coronary arteries and their connexions with the arterial trunks. *Int J Cardiol* 1988;**20**:117–123.
43. Waldo K, Willner W, Kirby M. Origin of the proximal coronary artery stems and a review of ventricular vascularization in the chick embryo. *Am J Anat* 1990;**188**: 109–120.
44. Ito WD, Arras M, Scholz D, Winkler B, Htun P, Schaper W. Angiogenesis but not collateral growth is associated with ischemia after femoral artery occlusion. *Am J Physiol* 1997;**273**:H1255–H1265.
45. Herzog S, Sager H, Khmelevski E, Deylig A, Ito WD. Collateral arteries grow from preexisting anastomoses in the rat hindlimb. *Am J Physiol Heart Circ Physiol* 2002;**283**: H2012–H2020.
46. Schaper W. [Development of collateral circulation in coronary artery occlusions]. *Deutsche Medizinische Wochenschrift* 1974;**99**:2299–2302.